

Observation of electric current induced by optically injected spin current

Xiao-Dong Cui^{a)}

Department of Physics, The University of Hong Kong, Hong Kong, China and Department of Chemistry, The University of Hong Kong, Hong Kong, China and HKU-CAS Joint Laboratory on New Materials, The University of Hong Kong, Hong Kong, China

Shun-Qing Shen^{a),b)} and Jian Li

Department of Physics, The University of Hong Kong, Hong Kong, China and Center of Theoretical and Computational Physics, The University of Hong Kong, Hong Kong, China

Yang Ji

SKLSM, Institute of Semiconductors, Chinese Academy of Sciences, P.O. Box 912, Beijing 100083, China

Weikun Ge

Department of Physics, The Hong Kong University of Science and Technology, Clear Water Bay, Hong Kong, China and Institute of Nano-Science and Technology, The Hong Kong University of Science and Technology, Clear Water Bay, Hong Kong, China

Fu-Chun Zhang

Department of Physics, The University of Hong Kong, Hong Kong, China and Center of Theoretical and Computational Physics, The University of Hong Kong, Hong Kong, China

(Received 3 May 2007; accepted 22 May 2007; published online 15 June 2007)

Linearly polarized light at normal incidence injects a spin current into a strip of two-dimensional electron gas with Rashba spin-orbit coupling. The authors report observation of an electric current when such light is shed on the vicinity of the junction in a crossbar-shaped InGaAs/InAlAs quantum well Rashba system. The polarization dependence of this electric current was experimentally observed to be the same as that of the spin current. The authors attribute the observed electric current to the scattering of the optically injected spin current at the crossing.

© 2007 American Institute of Physics. [DOI: 10.1063/1.2748843]

Optically injected spin current has been evidenced both in theory and experiments,¹⁻⁵ but detecting spin current, which is of great interest to spintronics physics as well as device applications, remains to be a challenging problem.⁶⁻¹³ A two-dimensional electron gas (2DEG) in a semiconductor heterostructure with C_{2v} symmetry and vertical structural inversion asymmetry (SIA) would induce a Rashba spin-orbit coupling and lead to spin splitting of the conduction band in the momentum space.^{14,15} This system provides a good platform for electrical control of electron spins in semiconductors. Such examples include spin photocurrent,¹ electric-dipole-induced spin resonance,¹⁶ and spin coherent transport.¹⁷ Among these efforts, optical injection of electron spin into 2DEG can be regarded as an efficient source to implement spin transport. Experimentally, the spin photogalvanic effect has been observed and studied extensively.^{2,3} In that effect, electrons in the valence band are pumped into the conduction band by irradiation of circularly polarized light, and the nonuniform distribution of the excited electrons due to the spin-orbit coupling will circulate a spin polarized electric current. In the case that the incident light is normal to the 2D plane, electrons with opposite spins would travel in opposite directions. As a result, a pure spin current circulates while the electric photocurrent vanishes.^{4,5}

In this letter, we report an observation of onward or outward electric currents in a crossbar-shaped [001] InGaAs/InAlAs quantum well when linearly polarized light irradiates on the sample at normal incidence near the junction at 77 K. The electric current was demonstrated to share the same light polarization dependence as the spin current. We attribute the observed electric current to the scattering of optically injected spin current in the crossing region.

The experimental setup is shown in Fig. 1(a), with a crossing bar carved on a sample of 2DEG which is formed at one interface between the only doped barrier and a 14 nm thick $\text{In}_{0.65}\text{Ga}_{0.35}\text{As}/\text{In}_{0.52}\text{Al}_{0.48}\text{As}$ quantum well (QW) grown on a semi-insulating [001] InP substrate by molecular beam epitaxy. The SIA was achieved by δ doping on the top of the well. The carrier density and mobility are about 1.5

$\times 10^{18} \text{ cm}^{-3}$ and $1000 \text{ cm}^2/\text{Vs}$, respectively. The spin coherence length is estimated to lie between the width of the narrow and wide channels.

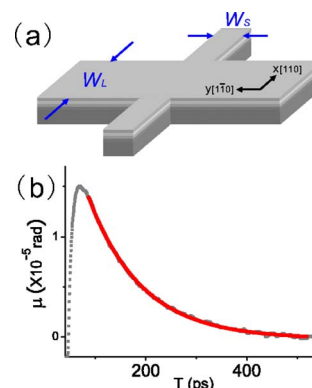


FIG. 1. (Color online) (a) Schematic view of the 2DEG sample and the experimental setup. The $20 \mu\text{m}$ and $200 \mu\text{m}$ wide planar channels are carved out by standard photolithography and wet etching. (b) Time-resolved Kerr rotation measurement finds a spin decoherence time of 106 ps. Black line: experimental data; red line: fitting with a single exponential function $\exp[-t/\tau_d]$. The spin coherence length is estimated to lie between the width of the narrow and wide channels.

^{a)} Author to whom correspondence should be addressed.

^{b)} Electronic mail: sshen@hkucc.hku.hk

$\times 10^{12} \text{ cm}^{-2}$ and $1.1 \times 10^5 \text{ cm}^2/\text{V s}$, respectively, determined by Hall measurement. The Rashba coupling coefficient is about $\alpha = 3.0 \times 10^{-12} \text{ eV m}$ determined by Shubnikov–de Hass oscillation.¹⁸ The time-resolved Kerr rotation measurement with standard pump probe technique gives the spin decoherence time $\tau_s \approx 106 \text{ ps}$ at 77 K, as shown in Fig. 1(b). The Fermi velocity of the sample is estimated to be $v_F \approx 5.0 \times 10^5 \text{ m/s}$ (taking the effective mass as $0.07m_e$). Thus the spin coherence length is roughly estimated to be $l_s \approx 53 \mu\text{m}$ at 77 K. Taking into consideration of these parameters, we designed a setup with two electric channels of widths $W_S = 20 \mu\text{m}$ and $W_L = 200 \mu\text{m}$, respectively, one being narrower and the other wider than the spin coherence length, i.e., $W_S/2 < l_s < W_L/2$, as shown in Fig. 1(a). The planar electric channels were carved out by standard photolithography and wet etching along the $[110]$ and the $[1\bar{1}0]$, defined as lab x and y axis, respectively [see Fig. 1(a)]. Electric contacts were made to the 2DEG by Ni/Au metal electrodes at far ends of the electric channels.

Linearly polarized laser light of wavelength of 880 nm and power of 40 mW produced by a tunable Ti:sapphire laser was used as the exciting source for the interband transition. The incident light was firstly guided through a photoelastic modulator (PEM), which modulated the light polarization to be oscillating between two orthogonal directions with a frequency of 50 kHz. Then the light was focused through a $10 \times$ objective lens before being normally shed upon a $10 \mu\text{m}$ diameter spot on the sample which was mounted in a cryostat at liquid nitrogen temperature. The electric currents passing through the terminals were monitored by voltage drops at symmetrically loaded resistors of 633Ω . The voltages were readout with a lock-in amplifier, which was triggered by the PEM so that the electric currents induced by nonpolarization related phenomena, e.g., Demer effect and thermoelectric effects, were clearly eliminated.

No measurable current along the wide channels (y axis) was observed on the background noise of tens of picoamperes under normal incidence, though a significant photocurrent was observed if the circular polarized light was shed at an oblique angle on the same samples.¹⁸ However, when linearly polarized light along the x or y axis was normally incident onto the plane near the electric channel junction, as illustrated in Fig. 2(a), we observed reproducible currents along the narrow channels under unbiased conditions. Figures 2(c)–2(e) show the currents passing through the terminals as functions of the spot position when the incident light is along the $20 \mu\text{m}$ wide channel (x axis). The current peaks at $x=0$ and $200 \mu\text{m}$ corresponding to the positions of the two channel junctions and vanishes at a distance of $50 \mu\text{m}$ away from the peak position. Note that the current curves of I_{C-A} and I_{C-B} and of I_{A-D} and I_{D-B} almost overlap, indicating that the current flows inward or outward simultaneously through the channel junction. The spatial distribution of the observed current is substantially different from the current due to Hall effect or the reciprocal spin Hall effect, where the Hall current is unidirectional. The flow pattern of the currents and the absence of a net electric current along the wide channel are the signatures of the observed effect, as summarized in Fig. 2(b). The vanishing of all currents at the middle point of the C-D channel, $x=100 \mu\text{m}$, evidently indicates that the phenomena are not due to conventional photocurrents.

As the current measurements were locked at the polarization oscillating frequency, the obtained current measures

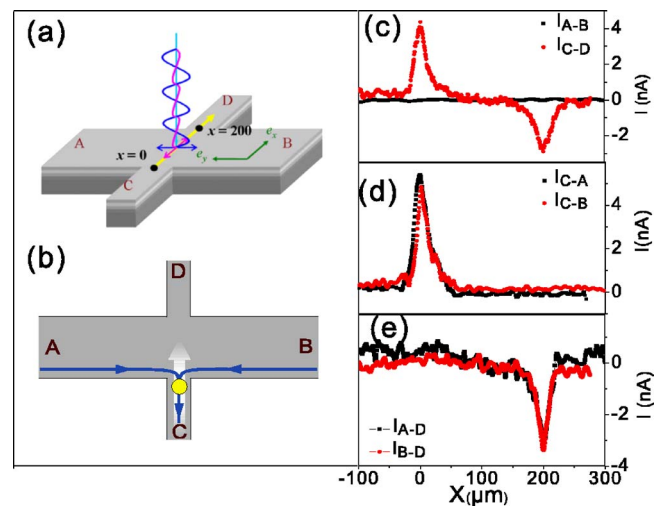


FIG. 2. (Color online) (a) Linearly polarized light beam, polarized along x axis as indicated by red color or along y axis as indicated by blue color, scans along the narrow channel (x axis) at normal incidence. (b) Flow pattern of measured electric currents for light spot along the narrow channel. [(c)–(e)] Typical charge currents through all the terminals as a function of the light spot position at x axis.

the difference between the electric currents generated by the two orthogonally polarized lights in the device. To further examine the relationship between the observed currents and polarization of the incident light, we rotate the polarization plane of the incident light while the light spot is fixed at the peak positions of I_{C-A} and I_{C-B} in Fig. 2(c). The current varies with the angle Φ between the light polarization plane and the y axis, and a good fit is obtained with the form $\cos 2\Phi$, as shown in Fig. 3. Obviously the polarization dependence of the current is in excellent agreement with the calculated angle dependence of the spin current.^{5,19}

The result of the laser scanning along the edge of channel A-B at $x=10 \mu\text{m}$ is shown in Fig. 4. Electric currents I_{A-C} and I_{B-C} were observed near the channel junction, and they were almost identical. The current I_{A-B} remains negligible despite the laser spot position moving, while the currents I_{A-D} and I_{B-D} also remain negligible since the light spot is located far away from the channel D. When the laser scans along the central line of channel A-B, i.e., at $x=100 \mu\text{m}$, no current was observed, for the light spot is located well beyond the spin coherence distance. This is consistent with the conventional spin photogalvanic effect, where the current vanishes when the linearly polarized light falls normally on the plane. We thus conclude that the observed electric current

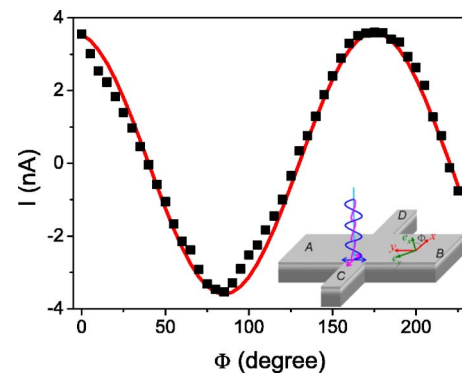


FIG. 3. (Color online) Charge current I_{A-C} (black square) at channel junction $x=0$ varies with the polarization angle Φ of light relative to the lab frame, as shown in the inset. The red curve is a fit of $\cos 2\Phi$.

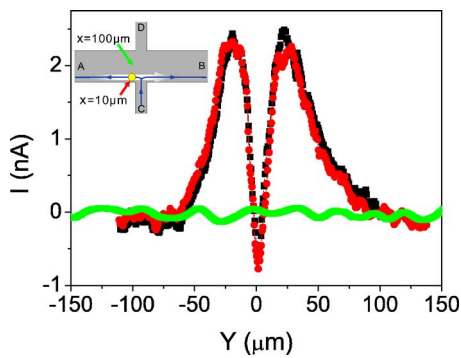


FIG. 4. (Color online) Charge currents I_{A-C} (red) and I_{B-C} (black) show strong position dependence when the light scans along $x=10 \mu\text{m}$. The current I_{A-C} (green) is negligible when the light scans along $x=100 \mu\text{m}$. The inset is the flow pattern of measured electric current for light spot scanning along the edge.

near the junction with a narrow width ($20 \mu\text{m}$) is not a conventional photocurrent.^{1,2,18} The equality of I_{A-C} and I_{B-C} obviously excludes the possibility of a diffusion mechanism for generating the photocurrent.

To understand the experimental results, we interpret the observed electric current as a result of the scattering of the spin current near the junction of the crossing bars. Firstly, the optical excitation serves as the source of a spin current with its spin polarization lying in the plane and perpendicular to the direction of the electron motion. The effective distance of this spin current is estimated to be within l_s , which has the relation of $W_S/2 < l_s < W_I/2$. Keeping this picture in mind the observed effect can then be well understood as follows. In the case that the light spot scans along the central line of the narrow channel C-D in Fig. 2, the geometric boundaries of the sample set a limit to the motion of the excited electrons and lead them to two opposite directions with opposite in-plane spin polarizations. Two beams of the excited electrons compose the same spin current, which is then scattered by the edges of the crossing region to produce a transverse electric current. On the other hand, when the light spot scans along the central line of the wide channel A-B in Fig. 4, the spin current decays to zero before it reaches the edges of the crossing region, therefore no electric current circulates. While in the case that the light spot moves along the edge, also shown in Fig. 4, when the distance between the spot and the edge is within l_s , the edge may again impose a constraint to the movement of the electrons and lead to an outward (inward) electric current along the edge, together with an inward (outward) electric current perpendicular to the edge, and thus a measurable current between C-A/C-B or D-A/D-B. Also as the spin coherence length at liquid nitrogen temperature is longer than the width $W_S=20 \mu\text{m}$ of the narrow channel, the impurity effect or other interactions would not be crucial in this experiment.

The conversion of spin current to electric current has been discussed extensively in the context of the reciprocal spin Hall effect where the separated spins are out of plane.²⁰ In the present case the spin current is polarized within the plane, as the linearly polarized light does not generate out-of-plane spin polarization due to conservation of the total angular momentum. As examined in Ref. 5, an electron of spin $-y$ polarization will be equally scattered along the x and $-x$ axes, and hence the resulted scattered electric current has such a pattern: either both outward or both inward, in the transverse directions of the spin current. Our experimental

observation of the electric currents is in excellent qualitative agreement with this picture. For the case of the in-plane-polarized spin current as in the present experiment, the conversion rate for the spin current to electric current is estimated to be 0.3%–1%.⁵ Although there are some unknown parameters of the sample, the amplitude of the injected spin current J_{xy} by the linearly polarized light can be roughly estimated by using the measurable photocurrent J_x injected by the circularly polarized light at a small oblique angle Θ away from normal. A theoretical estimation gives $J_x(\Theta)/J_{xy} \approx 0.17\Theta(2e/\hbar)$ by solving of semiconductor Bloch optical equation near the Γ point of the InGaAs 2DEG.¹⁹ Taking the light spot size, the geometry of the setup, and the laser power into account, we estimate from the experimental data that $J_x(\Theta) \approx 94\Theta \text{ nA}$ (Ref. 18) hence the injected spin current is estimated to be approximately 550 nA ($\hbar/2e$). The observed electric current is several nanoamperes, say, 4.0 nA for the peaks in Fig. 2(c). The conversion rate from the spin current to charge current is roughly about 0.8%, close to the numerically simulated values.

The authors thank S. J. Xu, L. Ding, and X. Z. Ruan for assistance in laboratory facility and X. Dai, J. Wang, B. Zhou, S. C. Zhang, and Q. Niu for helpful discussions. This work was supported by the Research Grant Council of Hong Kong under Grant No. HKU 7039/05P, the Large-Item-Equipment Funding and the University Development Funding of HKU on “Nanotechnology Research Institute” program under Contract No. 00600009.

¹S. D. Ganichev, E. L. Ivchenko, V. V. Bel’kov, S. A. Tarasenko, M. Sollinger, D. Weiss, D. Wegscheider, and W. Prettl, *Nature (London)* **417**, 153 (2002).

²For spin photocurrent, see S. D. Ganichev and W. Prettl, *J. Phys.: Condens. Matter* **15**, R935 (2003).

³S. D. Ganichev, E. L. Ivchenko, S. N. Danilov, J. Eroms, D. Wegscheider, D. Weiss, and W. Prettl, *Phys. Rev. Lett.* **86**, 4358 (2001).

⁴R. D. R. Bhat, F. Nastos, Ali Najmaie, and J. E. Sipe, *Phys. Rev. Lett.* **94**, 096603 (2005).

⁵J. Li, X. Dai, S. Q. Shen, and F. C. Zhang, *Appl. Phys. Lett.* **88**, 162105 (2006).

⁶J. Hubner, W. W. Rühle, M. Klude, D. Hommel, R. D. R. Bhat, J. E. Sipe and H. M. van Driel, *Phys. Rev. Lett.* **90**, 216601 (2003).

⁷M. J. Stevens, A. L. Smirl, R. D. R. Bhat, Ali Najmaie, J. E. Sipe, and H. M. van Driel, *Phys. Rev. Lett.* **90**, 136603 (2003).

⁸Y. K. Kato, R. C. Myers, A. C. Gossard, and D. D. Awschalom, *Science* **306**, 1910 (2004); V. Sih, R. C. Myers, Y. K. Kato, W. H. Lau, A. C. Gossard, and D. D. Awschalom, *Nat. Phys.* **1**, 31 (2005).

⁹J. Wunderlich, B. Kaestner, J. Sinova, and T. Jungwirth, *Phys. Rev. Lett.* **94**, 047204 (2005).

¹⁰E. Saitoh, M. Ueda, and H. Miyajima, *Appl. Phys. Lett.* **88**, 182509 (2006).

¹¹S. A. Wolf, D. D. Awschalom, R. A. Buhrman, J. M. Daughton, S. von Molnar, M. L. Roukes, A. Y. Chtchelkanova, and D. M. Treger, *Science* **294**, 1488 (2001).

¹²*Semiconductor Spintronics and Quantum Computation* edited by D. D. Awschalom, D. Loss, and N. Samarth (Springer, Berlin, 2002), Chap. 1, p. 1.

¹³I. Žutić, J. Fabian, and S. Das Sarma, *Rev. Mod. Phys.* **76**, 323 (2004).

¹⁴Y. A. Bychkov and E. I. Rashba, *J. Phys. C* **17**, 6039 (1984).

¹⁵R. Winkler, *Spin-Orbit Coupling Effects in Two Dimensional Electron and Hole Systems* (Springer, Berlin, 2003), Chap. 6, p. 67.

¹⁶M. Duckheim and D. Loss, *Nat. Phys.* **2**, 195 (2006).

¹⁷S. A. Crooker, M. Furis, X. Lou, C. Adelman, D. L. Smith, C. J. Palmström, and P. A. Crowell, *Science* **309**, 2191 (2005).

¹⁸C. L. Yang, H. T. He, L. Ding, L. J. Cui, Y. P. Zeng, and W. K. Ge, *Phys. Rev. Lett.* **96**, 186605 (2006).

¹⁹B. Zhou and S. Q. Shen, *Phys. Rev. B* **75**, 045339 (2007).

²⁰E. M. Hankiewicz, J. Li, T. Jungwirth, Q. Niu, S. Q. Shen, and J. Sinova, *Phys. Rev. B* **72**, 155305 (2005).